Chinese Chemical Letters 35 (2024) 109509

Contents lists available at ScienceDirect

Chinese Chemical Letters

journal homepage: www.elsevier.com/locate/cclet

Pillar[5]arene based artificial light-harvesting supramolecular polymer for efficient and recyclable photocatalytic applications

Lei Zhou[a,b,1], Youjun Zhou[b,1], Lizhen Fang[a,b,1], Yiqiao Bai[b], Yujia Meng[b], Liang Li[a,*],
Jie Yang[c,*], Yong Yao[b,*]

[a] *School of Chemical and Environmental Engineering, Shanghai Institute of Technology, Shanghai 201418, China*
[b] *School of Chemistry and Chemical Engineering, Nantong City Key Laboratory of Life-Organic Chemistry, Nantong University, Nantong 226019, China*
[c] *College of Science, Nanjing Forestry University, Nanjing 210037, China*

ARTICLE INFO

Article history:
Received 15 November 2023
Revised 2 January 2024
Accepted 10 January 2024
Available online 15 January 2024

Keywords:
Pillar[5]arenes
Light-harvest
Supramolecular polymer
Photosynthesis
Orthogonal self-assembly

ABSTRACT

Photosynthesis is the process through which living plants utilize photosynthetic pigments, such as chlorophyll, to convert CO_2 and water into organic compounds and release O_2 under visible light. In this study, we have successfully constructed a fluorescent supramolecular polymer (**P5Py**$_2$/Zn/**Gen**)n by employing orthogonal pillar[5]arene-based molecular recognition and metal ion coordination. Within the supramolecular polymer, the guest molecule **Gen** unit acts as a light-harvesting moiety, as the ACQ effect is inhibited by host-guest interactions, while the (**Py**)$_2$/Zn center serves as a catalytic site. By employing this orthogonal self-assembly strategy, we have enhanced the stability of both the donor and acceptor in catalyzing the reduction of *p*-nitrophenol to *p*-aminophenol. Moreover, this photocatalyst can be reused at least 5 times without significant conversion loss. These findings provide a pathway for constructing a recyclable artificial LHS that mimics the entire photosynthesis process.

Photosynthesis is the fundamental process by which living plants utilize photosynthetic pigments, like chlorophyll, to convert CO_2 and water into organic compounds while releasing O_2 in the presence of visible light [1]. During this process, chlorophyll molecules self-assemble into dense arrays, enabling them to capture energy from sunlight and concentrate it in reaction centers for conversion into chemical energy [2]. Drawing inspiration from natural photosynthesis, scientists have developed various artificial light-harvesting systems (LHSs) that not only enhance our understanding of photoinduced electron transfer and energy transfer in photosynthesis, but also have the potential to address global energy challenges through the development of clean and sustainable energy sources [3–6]. However, the dense arrangement of chromophores can result in fluorescence quenching due to the phenomenon known as aggregation-caused quenching (ACQ), which decreases the efficiency of energy capture [7–9]. In recent years, scientists have pursued two main strategies to suppress the ACQ effect. The first approach involves designing and synthesizing molecules with aggregation-induced emission (AIE) properties as the donor. These molecules are nearly non-fluorescent in their individual states but exhibit high fluorescence emission when they aggregate [10–13]. For instance, Zhang *et al.* reported the construction of an artificial LHS co-assembly using a tetraphenylethylene (TPE)-based Pt(II)-cage as the donor and Eosin Y as the acceptor for photocatalysis [10]. The second strategy involves exploiting host-guest interactions between the donor and macrocyclic hosts. These interactions effectively prevent tight packing and promote fluorescence emission when the chromophores aggregate [14,15].

Pillar[5]arenes have emerged as highly popular supramolecular macrocyclic hosts in the last decade [16–18]. Their unique structure, which features ten phenolic hydroxyl groups that can be easily modified, allows for the preparation of various derivatives [19–22]. The rigid and symmetrical cavity of pillar[5]arenes further enhances their exceptional host-guest properties [23–27]. Consequently, significant advancements have been made in the synthesis [28–30], functionalization [31–33], host-guest properties in different solvents, and diverse applications of pillar[5]arenes over the past decade [34–39]. Notably, their application in supramolecular polymers has garnered significant attention from both chemistry and materials scientists [40–43].

It is worth noting that natural LHSs in living plants are formed through non-covalent interactions between chlorophyll and proteins. In contrast to traditional artificial LHSs constructed with co-

---

[*] Corresponding authors.

E-mail addresses: lilianglcx@sit.edu.cn (L. Li), jieyang@njfu.edu.cn (J. Yang), yaoyong1986@ntu.edu.cn (Y. Yao).

[1] These authors contributed equally to this work.

https://doi.org/10.1016/j.cclet.2024.109509

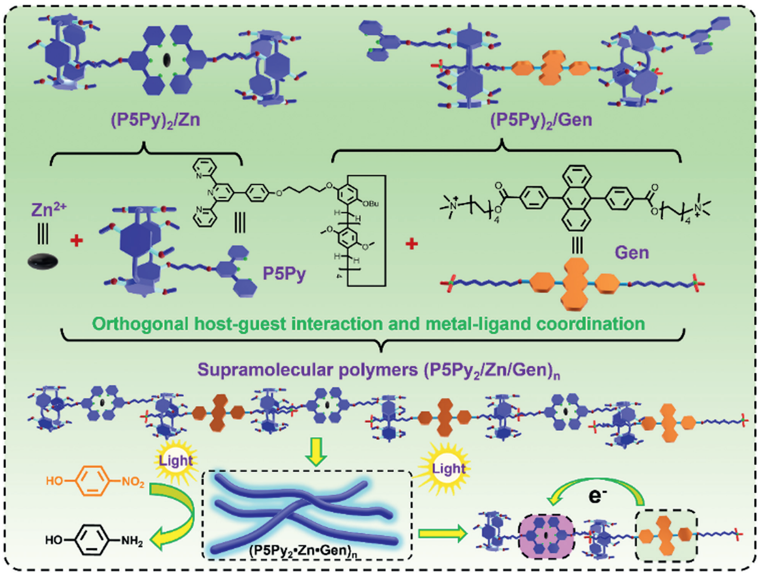

Scheme 1. Chemical structures of terpyridine-modified-pillar[5]arene (**P5Py**) and di(alkyl-trimethylammonium)-modified-anthracene (**Gen**) and cartoon representations of the artificial light-harvesting supramolecular polymers for photocatalytic reduction of nitro-aromatics.

valent bonds, supramolecular LHSs built through non-covalent interactions offer several advantages: they eliminate the need for multi-step synthesis and purification during structure construction, reduce costs, and enhance light conversion efficiency [44–48]. At present, most artificial supramolecular LHSs need to load additional receptors and donors, so it is a very meaningful work to develop different types of artificial supramolecular LHSs [49,50]. Considering the above points, we aimed to fabricate an efficient, recyclable artificial LHS that mimics the process of photosynthesis. To achieve this, we developed a fluorescent supramolecular polymer using orthogonal self-assembly, involving host-guest and metal coordination interactions (Scheme 1). The host-guest interaction effectively inhibits the ACQ effect, allowing the **Gen** unit to act as a light-harvesting moiety, while the (**Py**)$_2$/Zn center serves as a catalytic site. Moreover, this orthogonal self-assembly strategy enhances the stability of the donor and acceptor components in the system and improves the recyclability for catalyzing the reduction of *p*-nitrophenol to *p*-aminophenol.

Having obtained **P5Py** and **Gen**, we initially examined the interactions between Zn^{2+}, **P5Py**, and **Gen**. Previous reports have demonstrated that the terpyridine group and metal ions can form a stable metal complex [51]. NMR spectra analysis revealed that upon the addition of Zn^{2+} to **P5Py**, the chemical shift of H adjacent to N shifted to the low field. This shift suggests the formation of a coordination bond between the terpyridine unit and Zn^{2+} (Fig. S10 in Supporting information). Moreover, the absorbance of the terpyridine unit in the synthesized **P5Py** showed a gradual shift from 290 nm to 330 nm, further indicating the complexation between Zn^{2+} ions and the terpyridine unit (Fig. 1a). By employing UV–vis titrations, the coordination constant (K_a) of **P5Py** with Zn^{2+} was calculated to be $(1.58 \pm 0.32) \times 10^4$ L/mol (Fig. S11 in Supporting information). Furthermore, it was observed that the stoichiometry between **P5Py** and Zn^{2+} was 2:1 (Fig. 1b, Figs. S11c and S12 in Supporting information). On the other hand, alkyl trimethylammonium could penetrate into the cavity of pillar[5]arene to form host-guest complex, which can be confirmed by the ^{1}H NMR from model pillar[5]arene and guest (Fig. S13 in Supporting information). The association constant (K_b) between **Gen** and **P5Py** was determined to be $(1.51 \pm 0.23) \times 10^4$ L/mol through fluorescent titrations (Fig. S14 in Supporting information). From the fluorescence spectra of the system with different ratio of [**Gen**]/[(**P5Py**)$_2$ Zn], the stoichiometry between (**P5Py**)$_2$ Zn and **Gen** was 1:1 (Figs. 1c and d).

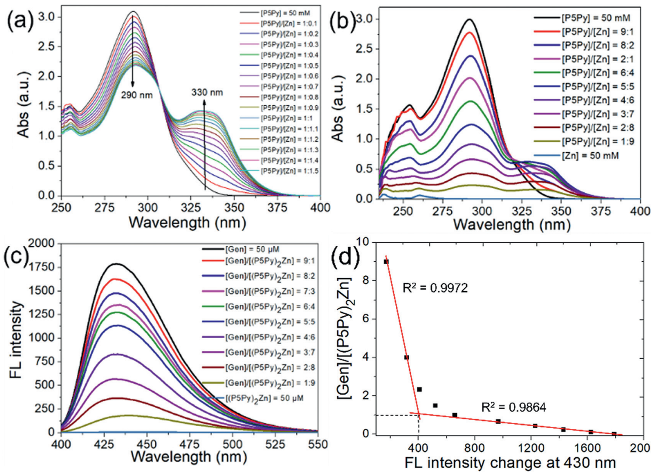

Fig. 1. (a) UV–vis absorption spectra of **P5Py** (50 mmol/L) upon addition of $Zn(ClO_4)_2$ in DMF. (b) UV–vis absorption spectra of **P5Py** with different ratio of [**P5Py**]/[Zn]. ([**P5Py**] + [Zn] = 50 mmol/L. (c) Fluorescence spectra of the system with different ratio of [**Gen**]/[(**P5Py**)$_2$ Zn]. [**Gen**] + [(**P5Py**)$_2$ Zn] = 50 µmol/L, (λ_{ex} = 380 nm). (d) Mole ratio plot for (**P5Py**)$_2$ Zn and **Gen**, indicating a 1:1 stoichiometry.

After confirming orthogonal **P5Py**/Zn coordination and **P5Py**$_2$/**Gen** recognition motifs, the linear supramolecular polymer (**P5Py**$_2$/Zn/**Gen**)n was initially hypothesized to be driven by host-guest interactions and metal coordination in CH_3CN. To confirm the formation of supramolecular polymers, viscometry and 2D diffusion-ordered ^{1}H NMR spectroscopy (DOSY) was employed. The viscosity transition of the assembled linear supramolecular polymer A was observed using double logarithmic plots of specific viscosity *versus* concentration, as depicted in Fig. S15 (Supporting information). In the low concentration range, the slopes approximated unity, indicating the presence of cyclic oligomers with a constant size. However, when the concentration surpassed the critical polymerization concentration (CPC; approximately 60.0 mmol/L), a sharp increase in viscosity was observed. Moreover, the morphology of the supramolecular polymers was examined using scanning electron microscopy

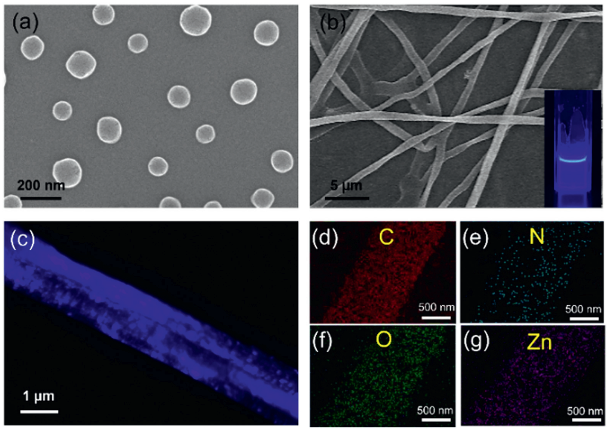

Fig. 2. (a) SEM images of (**P5Py₂**/Zn/**Gen**)n when the concentration is 20 mmol (a) and 100 mmol (b). (c) Fluorescence microscope of (**P5Py₂**/Zn/**Gen**)n at 100 mmol. (d-g) EDS mapping images of (**P5Py₂**/Zn/**Gen**)n.

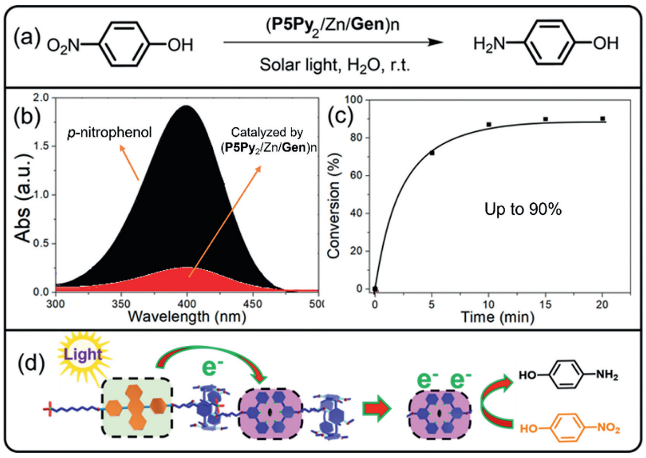

Fig. 3. (a) Catalyst comparison using artificial (**P5Py**$_2$/Zn/**Gen**)n and **Zn**/**Gen** as photocatalysts for reduction *p*-nitrophenol. (b) UV–vis absorption of *p*-nitrophenol reduced by (**P5Py**$_2$/Zn/**Gen**)n after 20 min. (c) Conversation of *p*-nitrophenol *versus* reaction time. (d) Mechanism of reducing *p*-nitrophenol using (**P5Py**$_2$/Zn/**Gen**)n as photocatalyst.

(SEM). As shown in Fig. 2a, (**P5Py**$_2$/Zn/**Gen**)n self-assembled into nanoparticles with diameters ranging from 120 nm to 200 nm at a concentration of around 20 mmol. Above the CPC, a rod-like fiber with a regular diameter of 1 μm was observed by SEM (Fig. 2b). Notably, both the fluorescent picture (Fig. 2b, inset) and fluorescent microscopy image (Fig. 2c) demonstrated that the obtained (**P5Py**$_2$/Zn/**Gen**)n polymer emitted bright blue light. Furthermore, SEM-energy-dispersive X-ray (EDX) mapping technology revealed the homogeneous dispersion of C, N, O, and Zn throughout the polymers (Figs. 2d–g).

Table 1
Photocatalytic reduction of nitroaromatic compounds by our LHSs at room temperature.

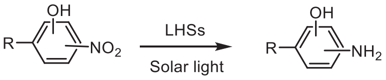

Substrate	Solvent	Time (h)	Conversion (%)
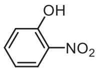	Water	2	85.6
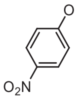	Water	2	94.2
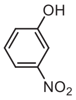	Water	2	92.9
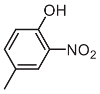	Water	2	87.1
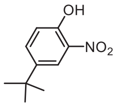	Water	2	87.3
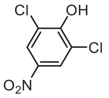	DMF:water = 1:10	2	92.3
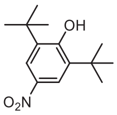	DMF:water = 1:10	2	91.7

As depicted in Fig. S16 (Supporting information), the fluorescence intensity of **Gen** decreased as the concentration increased. However, when addition of **P5Py**, the fluorescence will increase. This is due to the dense arrays of anthracene units were inhibited by the host-guest interaction between pillar[5]arene and the alkyl-trimethylammonium group. Consequently, the supramolecular polymer did not exhibit the ACQ effect, resulting in its bright blue fluorescence. This property enabled the (**P5Py**$_2$/Zn/**Gen**)n supramolecular polymer to function as a photocatalyst for the reduction of *p*-nitrophenol, mimicking the process of photosynthesis (Fig. 3a). As shown in Fig. 3b, the absorption of *p*-nitrophenol decreased rapidly when (**P5Py**$_2$/Zn/**Gen**)n was used as the catalyst. After a 20-min reaction, the conversion of *p*-nitrophenol reached 90.3% using the LHS as the photocatalyst. The mechanism behind the photocatalytic reaction involves the LUMO energy level of (**Py**)$_2$ Zn being closer to, but lower than, the anthracene unit, facilitating the transfer of excited-state electrons from the anthracene core to the (**Py**)$_2$ Zn center (Fig. S17 in Supporting information) [51]. Subsequently, *p*-nitrophenol can be reduced to 4-aminophenol by the electrons on the surface of the (**Py**)$_2$/Zn center (Fig. 3d).

Most acceptors, such as Eosin Y, are typically loaded into artificial supramolecular LHSs through hydrophobic interactions, which makes them challenging to reuse in the process of mimicking photosynthesis [49]. In contrast, our (**P5Py**$_2$/Zn/**Gen**)n-based LHS incorporates the light-harvesting unit and catalytically active moiety through orthogonal pillar[5]arene-based molecular recognition and metal ion coordination. This unique approach enhances the stability of the system during photocatalysis. As illustrated in Fig. 4a, (**P5Py**$_2$/Zn/**Gen**)n can be reused at least 5 times without significant loss of activity in the photocatalytic reduction of 4-nitrophenol (<3% conversion loss). Elemental mapping analysis (Figs. 4b–f) of (**P5Py**$_2$/Zn/**Gen**)n after five cycles of reuse revealed homogeneous distributions of N, O, and Zn across the polymer, confirming the stability of (**P5Py**$_2$/Zn/**Gen**)n throughout the reaction process.

With (**P5Py**$_2$/Zn/**Gen**)n-based LHS in hand, we then evaluated the photocatalyst's ability to reduce nitro-aromatics. Specifically, we investigated the effect of substituent type and position on the reaction using 2-nitrophenol, 4-nitrophenol, 3-nitrophenol, 4-methyl-2-nitrophenol, 4-*tert*–butyl-2-nitrophenol, 2,6-dichloro-4-nitrophenol, and 2,6-di-*tert*–butyl-4-nitrophenol (Fig. S18 in Supporting information). As shown in Table 1, all the substrates were successfully reduced to the corresponding amino-phenols with significant conversion. For instance, *meta*- and *para*-nitrophenol ex-

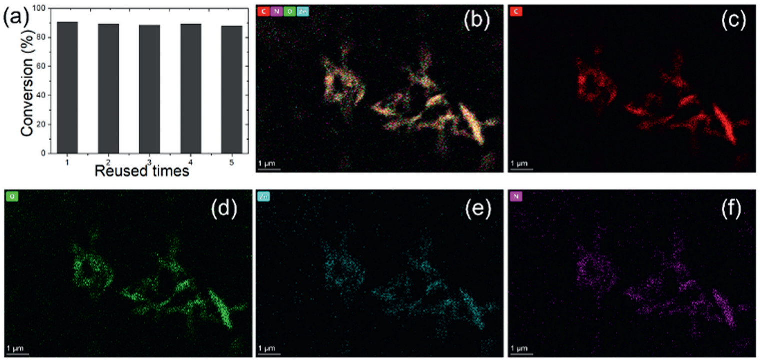

Fig. 4. (a) Conversion of 4-nitrophenol to 4-aminophenol catalyzed by artificial (**P5Py$_2$**/Zn/**Gen**)n against cycle times. (b-f) EDS mapping images of (**P5Py$_2$**/Zn/**Gen**)n after reusing 5 times.

hibited a conversion greater than 90%. Additionally, 2-nitrophenol and *para*-alkyl (−Me, *t*Bu)-substituted 2-nitrophenol demonstrated a photocatalytic conversion rate of 85.6%–87.3%. It is worth noting that 2,6-dichloro-4-nitrophenol and 2,6-di-*tert*-butyl-4-nitrophenol were dissolved in a DMF/water mixture and exhibited conversions of 91.7% and 92.3% respectively. These results confirmed the versatility of our (**P5Py**$_2$/Zn/**Gen**)n-based LHS as a general photocatalyst for the reduction of nitro-aromatics.

In conclusion, we successfully constructed a fluorescent supramolecular polymer (**P5Py**$_2$/Zn/**Gen**)n using orthogonal pillar[5]arene-based molecular recognition and metal coordination. Various characterization techniques, including DOSY, UV–vis spectroscopy, fluorescence spectroscopy, viscosity measurements, SEM imaging, and EDS mapping, were employed to investigate the properties of the obtained polymers. In this supramolecular polymer, the host-guest interactions effectively suppress the ACQ effect of **Gen** units, allowing them to function as efficient light-harvesting moieties even at high concentrations. Meanwhile, the (**Py**)$_2$/Zn center acts as a catalytic site. This orthogonal self-assembly strategy enhances the stability and recyclability of our (**P5Py**$_2$/Zn/**Gen**)n in catalyzing the reduction of *p*-nitrophenol to *p*-aminophenol. This study presents a promising approach to design a recyclable artificial LHS that mimics the complete process of photosynthesis.

Declaration of competing interest

The authors declare that they have no known competing financial interests or personal relationships that could have appeared to influence the work reported in this paper.

Acknowledgments

This work was supported by the National Natural Science Foundation of China (Nos. 32101215, 22007052), Natural Science Foundation of Jiangsu Province (Nos. BK20180942, BK20190917). We also thank Nantong University Analysis & Testing Center for characterization.

Supplementary materials

Supplementary material associated with this article can be found, in the online version, at doi:10.1016/j.cclet.2024.109509.

References

[1] B. Zhang, L. Sun, Chem. Soc. Rev. 48 (2019) 2216–2264.
[2] G.D. Scholes, G.R. Fleming, A. Olaya-Castro, R. van Grondelle, Nat. Chem. 3 (2011) 763–774.
[3] J.K. McCusker, Science 363 (2019) 484–488.
[4] T. Xiao, W. Zhong, L. Zhou, et al., Chin. Chem. Lett. 30 (2019) 31–36.
[5] Z. Yu, H.K. Bisoyi, X.-M. Chen, et al., Angew. Chem. Int. Ed. 61 (2022) e202200466.
[6] J. Xu, B. Zhang, M. Jansen, et al., Angew. Chem. Int. Ed. 56 (2017) 13882–13886.
[7] Y. Zeng, Y. Li, M. Li, G. Yang, Y. Li, J. Am. Chem. Soc. 131 (2009) 9100–9106.
[8] F.C. De Schryver, T. Vosch, M. Cotlet, et al., Acc. Chem. Res. 38 (2005) 514–522.
[9] X. Zhang, Y. Zeng, T. Yu, et al., Phys. Chem. Lett. 5 (2014) 2340–2350.
[10] Z. Zhang, Z. Zhao, Y. Hou, et al., Angew. Chem. Int. Ed. 58 (2019) 8862–8866.
[11] J. Yang, Z. Chi, W. Zhu, B.Z. Tang, Z. Li, Sci. China Chem. 62 (2019) 1090–1098.
[12] K. Acharyya, S. Bhattacharyya, H. Sepehrpour, et al., J. Am. Chem. Soc. 141 (2019) 14565–14569.
[13] S. Fu, X. Su, M. Li, et al., Adv. Sci. 7 (2020) 2001909.
[14] T. Chen, J. Wang, R. Tang, et al., Chin. Chem. Lett. 34 (2023) 108088.
[15] H. Guo, X. Yan, B. Lu, et al., J. Mater. Chem. C 8 (2020) 15622–15625.
[16] T. Ogoshi, T.-a. Yamagishi, Y. Nakamoto, Chem. Rev. 116 (2016) 7937–8002.
[17] R. Tang, Y. Ye, S. Zhu, et al., Chin. Chem. Lett. 34 (2023) 107734.
[18] M. Wang, Q. Li, E. Li, et al., Angew. Chem. Int. Ed. 60 (2021) 8115–8120.
[19] S. Fa, K. Adachi, Y. Nagata, et al., Chem. Sci. 12 (2021) 3483–3488.
[20] T. Xiao, L. Qi, W. Zhong, et al., Mater. Chem. Front. 3 (2019) 1973–1993.
[21] B. Hua, W. Zhou, Z. Yang, et al., J. Am. Chem. Soc. 140 (2018) 15651–15654.
[22] H. Liang, Y. Yang, L. Shao, et al., J. Am. Chem. Soc. 145 (2023) 2870–2876.
[23] M. Schmidt, B. Esser, Chem. Commun. 57 (2021) 9582–9585.
[24] H. Guo, J. Ye, Z. Zhang, et al., Inorg. Chem. 59 (2020) 11915–11919.
[25] L. Shao, Y. Pan, B. Hua, et al., Angew. Chem. Int. Ed. 59 (2020) 11779–11783.
[26] L. Shen, Y. Zhao, D. Dai, et al., Chem. Commun. 56 (2020) 1381–1384.
[27] B. Hua, L. Shao, Z. Zhang, J. Liu, F. Huang, J. Am. Chem. Soc. 141 (2019) 15008–15012.
[28] M. Bojtar, A. Simon, P. Bombicz, I. Bitter, Org. Lett. 19 (2017) 4528–4531.
[29] K. Kato, K. Maeda, M. Mizuno, et al., Angew. Chem. Int. Ed. 61 (2022) e202212874.
[30] C. Han, D. Zhao, Z. Lu, et al., Eur. J. Org. Chem. 14 (2019) 2508–2512.
[31] Y. Wang, R. Tang, Y. Zhang, et al., Inorg. Chem. 62 (2023) 7605–7610.
[32] M. Shin, S. Kim, E. Lee, et al., Inorg. Chem. 60 (2021) 5804–5811.
[33] W. Cui, L. Wang, L. Xu, et al., J. Phys. Chem. Lett. 9 (2018) 1047–1052.
[34] B. Jiang, W. Wang, Y. Zhang, et al., Angew. Chem. Int. Ed. 56 (2017) 14438–14442.
[35] R. Wang, Y. Sun, F. Zhang, et al., Angew. Chem. Int. Ed. 56 (2017) 5294–5298.
[36] M. Zhang, P.-P. Zhu, P. Xin, et al., Angew. Chem. Int. Ed. 56 (2017) 2999–3003.
[37] B. Shi, K. Jie, Y. Zhou, et al., J. Am. Chem. Soc. 138 (2016) 80–83.
[38] C. Fan, W. Wu, J.J. Chruma, J. Zhao, C. Yang, J. Am. Chem. Soc. 138 (2016) 15405–15412.
[39] J. Wang, M. Cen, J. Wang, et al., Chin. Chem. Lett. 33 (2022) 1475–1478.
[40] L. Xu, Z. Wang, R. Wang, et al., Angew. Chem. Int. Ed. 59 (2020) 9908–9913.
[41] P. Wang, B. Liang, D. Xia, Inorg. Chem. 58 (2019) 2252–2256.
[42] X. Zeng, H. Deng, X. Jia, et al., Chem. Commun. 54 (2018) 11634–11637.
[43] Y. Yao, Y. Sun, H. Yu, et al., Dalton Trans. 46 (2017) 16802–16806.
[44] S. Guo, Y. Song, Y. He, X.Y. Hu, L. Wang, Angew. Chem. Int. Ed. 57 (2018) 3163–3167.
[45] C.L. Sun, H.Q. Peng, L.Y. Niu, et al., Chem. Commun. 54 (2018) 1117–1120.
[46] T. Xiao, H. Qian, Y. Shen, et al., Mater. Today Chem. 24 (2022) 100833.
[47] H. Qian, T. Xiao, R.B.P. Elmes, L. Wang, Chin. Chem. Lett. 34 (2023) 108185.
[48] Z. Wu, H. Qian, X. Li, T. Xiao, L. Wang, Chin. Chem. Lett. 35 (2024) 108829.
[49] W.J. Li, X.Q. Wang, D.Y. Zhang, Angew. Chem. Int. Ed. 60 (2021) 18761–18768.
[50] L. Xu, R. Wang, H. Tang, L. Wang, D. Cao, J. Mater. Chem. A 10 (2022) 11332–11339.
[51] P. Verma, A. Singh, F.A. Rahimi, T.K. Maji, J. Mater. Chem. A 9 (2021) 13608–13614.